


 Cite this: *RSC Adv.*, 2021, **11**, 32459

Received 22nd July 2021
 Accepted 20th September 2021
 DOI: 10.1039/d1ra05605k
rsc.li/rsc-advances

Novel self-healing and multi-stimuli-responsive supramolecular gel based on D-sorbitol diacetal for multifunctional applications†

Fuqiang Wen,^a Jingjing Li,^b Lei Wang,^a Fei Li,^a Haiyang Yu,^a Binglong Li,^b Kaiqi Fan^b and Xidong Guan^{a*}

A simple-structured super gelator with self-healability and multi-stimuli responses was reported herein, which exhibited multiple visual molecular recognition abilities. Multifunctional applications such as effective lubricants, safe fuels, high-efficient propellants, dyes adsorbents, enhanced fluorescence emission and separation of aldehydes from aqueous solutions are integrated into a single organogelator, which was rarely reported.

Great achievements of supramolecular science have aroused an even more urgent need for seeking environmentally friendly next-generation functional materials to accelerate the development of adaptive green multifunctional materials for renewable and clean energy technologies.¹ As a class of stimuli-responsive soft matter, supramolecular gels have been considered as promising candidates for the next-generation of smart soft materials² with wide potential application, such as thixotropy,³ self-healing,⁴ visual molecular recognition,⁵ phase-selective gelation capacities⁶ and dye adsorption.⁷ Many attempts have been made to develop and utilize supramolecular gels as green functional materials due to their low toxicity, efficient reusability and low cost in various application processes. Supramolecular gel formation or collapse has been used for visual recognition of structural analogues, demonstrating a simple, low-cost, convenient and less-polluting recognition approach.⁵ Supramolecular alcogels have been reported as green fuels due to their advantages over the liquid alcohols such as safety easy handling, and delivery.⁸ Supramolecular oleogels have been utilized for effective lubricants⁹ and propellants,¹⁰ overcoming the problems related to spillage and safety of liquid lubricant and propellants which promotes to the sustainable development on the environment and the ecosystem. Supramolecular phase-selective gels (PSGs) have been proved to be highly efficient and environmentally friendly technique for the recovery of organic solvents and oils.¹¹ Xerogels of the supramolecular

hydrogels/organogels have been used as highly-efficient absorbents for wastewater treatment.¹² Although different types of supramolecular gels with different potential applications have been developed,¹³ there were few reports on the realization of multiple applications based on a single low-molecular-weight gelator (LMWG). This is because they need to perfectly combine the structure of the gelling agent with the environment of non-covalent interaction. Therefore, integrating multi-stimulus responses and multifunctional applications into a single LMWG is a real challenge because it can bring greater flexibility to the creation of smart materials.

Inspired by the progress of research work in the area of sugar-derived LMWGs, we decided to design a new supramolecular gel that contains multi-stimulus responses and multifunctional applications. Herein a new D-sorbitol diacetal gelator (D1) with methoxy group was synthesized (Fig. 1). The D1-based gels exhibited multiple visualized molecular recognition abilities such as discriminate enantiomer, metal ions and structural analogues (aliphatic amines and aromatic amines). Interestingly, The D1-based gels can be used not only as effective self-constraint gel lubricants with high phase transition temperature, safe and feasible fuels, but also as highly-efficient propellants and dyes adsorbents. Notably, the D1 gelator powder showed excellent phase-selective aldehyde liquids capacities at room temperature, whereas the xerogels of the D1

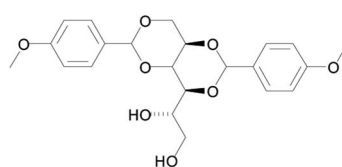


Fig. 1 Chemical structure of gelator D1.

^aSchool of Pharmaceutical Sciences, Shandong First Medical University, Shandong Academy of Medical Sciences, Tai'an 271016, China. E-mail: xidongguan@163.com

^bSchool of Chemistry and Chemical Engineering, Henan University of Technology, Zhengzhou 450001, China

^cCollege of Material and Chemical Engineering, Zhengzhou University of Light Industry, Zhengzhou 450002, P. R. China. E-mail: benlto@163.com

† Electronic supplementary information (ESI) available: Experimental details and supplementary figures. See DOI: 10.1039/d1ra05605k



displayed unexpected enhanced fluorescence of acid fuchsin. To the best of our knowledge, such versatile supramolecular gel materials have never been reported previously.

The gelator D1 was synthesized according to an already published method.¹⁴ First, the gelation abilities of D1 were examined in various solvents by the heating–cooling method (ESI, Table S1†). The D1 gelator showed outstanding gelation ability in protic and aprotic solvents as well as in various oils. For instance, the gelator formed gels in a series of alcoholic solvents, such as methanol, ethanol, *n*-propanol, isopropanol, *n*-butanol, *n*-octanol and iso-octanol. On the other hand, the critical gelator concentrations (CGCs) (ESI, Tab. S1†) for *o*-xylene and *o*-dichlorobenzene were lower than 0.1 wt%, which recommend the D1 gelator as a supergelator material.¹⁵ Interestingly, the gelator can solidify a variety of lubricating media, such as liquid paraffin, alkylated naphthalenes (ANs), 150BS, polyalphaolefin (PAO10), multiple-alkylated cyclopentane (MACS), and triethylene glycol. It also proved to be a good gelling agent for high-energy density hydrocarbon fuels (*e.g.* JP-10, C10H16, *exo*-tetrahydrodicyclopentadiene), which is a common propellant used for military or space purposes. These extraordinary gelation capacities make the D1-based gels very versatile for various applications, *e.g.* as effective lubricant, safe fuel, and high-efficient propellant, which will be demonstrated later in this text.

The self-assembly mechanism of the gelator was investigated by FT-IR and ¹H NMR spectroscopies. In the chloroform solution, the stretching band of –OH was observed at 3461 cm^{–1}, whereas it shifted to 3235 cm^{–1} in the acetonitrile xerogel (ESI, Fig. S5†), indicating that the O–H groups participated to the formation of hydrogen bonds network.¹⁶ To get more insight into the molecular arrangements during the gelation step, concentration and temperature-dependent ¹H NMR studies were performed in deuterated acetonitrile (ESI, Fig. S6†). It was observed that the O–H protons corresponding to 4.17 (H_c) and 4.12 (H_d) ppm downfield to 4.20 and 4.14 ppm as the concentration increased. These results clearly indicate the formation of intermolecular hydrogen bonds between various hydroxyl groups.¹⁶ Furthermore, as the temperature increased from 45 to 55 °C, the O–H protons were shifted upfield to 4.15 and 4.10 ppm for H_c and H_d, respectively, which was also reinforce the formation of intermolecular hydrogen bonds among hydroxyl protons during the gelation process.¹⁶ The aromatic protons appeared at 7.42 (H_a) and 6.93 (H_b) ppm at 25 °C. As temperature increased to 55 °C, the peaks slightly upfield to 7.41 and 6.90 ppm, respectively, suggesting the generation of intermolecular π–π stacking during the gel formation.^{17,18} The XRD patterns of the acetonitrile xerogels (ESI, Fig. S7†) showed d-spacing values of 1.51, 0.75, and 0.51 nm, in a ratio of 1 : 1/2 : 1/3, indicating an ordered layered arrangements.^{5a} SEM and TEM studies (ESI, Fig. S8†) revealed that the acetonitrile gel aggregated into fibers with an average diameter of 30 nm. These results demonstrate that organogelation self-assembly generated highly ordered fibrous structures through both hydrogen bonds and π–π stacking, which is in agreement with those reported in the literature.¹⁹

The organogel demonstrated unusual properties as multiple visual recognition properties due to the gel response to different chemical and physical stimuli. First, the organogel exhibited an enantioselective response toward D- or L-lactic acid. As shown in Fig. 2, addition of an equivalent amount of D-lactic acid on the top of gels of D1/(acetonitrile : acetone = 8 : 2, 1%, w/v), converted the gels into a solution after a heating–cooling cycle. In contrast, L-lactic caused the gel to remain stable under the same conditions. ¹H NMR and IR spectroscopy experiments were carried out to assess the chiral recognition mechanism (ESI, Fig. S9†). Upon the addition of L-lactic to gels of D1/(acetonitrile : acetone = 8 : 2), the O–H protons corresponding to 4.14 (H_c) and 4.10 (H_d) ppm shifted to 4.10 and 4.16 ppm while the addition of L-lactic caused the O–H protons moved to 4.05 and 4.01. It was observed that the addition of D-lactic caused a larger downfield shift than that of the L-lactic. The xerogel of D1/(acetonitrile : acetone = 8 : 2) showed stretching band of –OH at 3234 cm^{–1}. It was observed that the stretching band of –OH group for the xerogel with L-lactic was significantly shifted to 3406 cm^{–1} whereas it shifted to 3447 cm^{–1} in the xerogel with D-lactic. Xerogel with D-lactic also made a larger shift than L-lactic, which is in agreement with the ¹H NMR studies. These results demonstrate that the enantioselective response toward D- or L-lactic acid is caused by multiple hydrogen bonding interactions. The different shifts of OH show that D- or L-lactic acid exhibit different interaction ability to the gelator D1. The addition of D-lactic acid could easily penetrate the supramolecular skeleton and then interact with gelator through multiple hydrogen bonding interactions because of less steric hindrance between them. On the contrary, for L-lactic, a greater steric hindrance

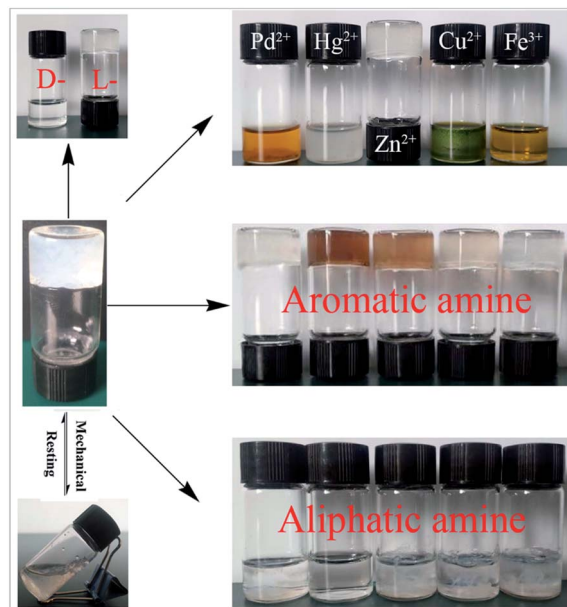


Fig. 2 The multiple visual recognition properties of D1 gels. D-: D-lactic acid, L-: L-lactic acid, aromatic and aliphatic amine from left to right: benzylamine, 4-phenetidine, 4-ethylaniline, 3-chloroaniline, *o*-toluidine and ethylamine, propylamine, *n*-butylamine, *n*-hexylamine *n*-octylamine respectively.



due to inconsistent chirality would lead to less interaction.²⁰ Based on above results, the mechanism of the molecular recognition of organogel was proposed and shown in Scheme S1.[†] Compared with L-lactic acid, D-lactic acid had a smaller steric hindrance and was easy to enter the nanofibers of the gel, destroy the interaction between the gel factors, and lead to the destruction of the gel. Thus, chiral selection was observed. In addition, the organogel also exhibits an efficient “naked eye” response to different metal ions by gel-sol transition and color changes. Addition of up to 0.5 eq. of cations, such as Pd^{2+} , Hg^{2+} , Zn^{2+} , Cu^{2+} and Fe^{3+} , on the top of the D1/acetonitrile gels converted the gels into a solution within 30 min, except Zn^{2+} , yielding a drastic colour change. The use of EDTA and methanol was not helpful for recovering the gel, suggesting the decomposition of the gelator by cations. 1H NMR experiments was performed to confirm this process. As shown in Fig. S10,[†] when the cations were added to acetonitrile gel, the signal of *p*-methoxybenzaldehyde appeared (9.89 ppm), indicating the decomposition of the diacetal in gelator. It was worth mentioning that the gel exhibited the visual discrimination of aliphatic and aromatic amines *via* gel-sol transition approach. As a result of addition of up to 1.0 eq. of aliphatic amines (ethylamine, propylamine, *n*-butylamine, *n*-hexylamine and *n*-octylamine) on the top of gels of D1/(acetonitrile : acetone = 8 : 2), promoted the transformation of the gel into suspension without recovering the gel, while aromatic amines (benzylamine, 4-phenetidine, 4-ethylaniline, 3-chloroaniline, *o*-toluidine) kept the gel remain stable. The gel collapse may be due to the addition of aliphatic amines resulted in the formation of $RNH \cdots HO$ hydrogen bonding and destroyed the original hydrogen bonding. 1H NMR spectroscopy was performed to monitor this process. As shown in Fig. S11 (ESI),[†] compared to the OH proton signal of D1 in 4.14 (H_c) and 4.10 (H_d) ppm in acetonitrile : acetone = 8 : 2, the signal shifted gradually downfield due to the formation of the $RNH \cdots HO$ hydrogen bonding. When 1 equivalents of ethylamine, propylamine, *n*-butylamine, *n*-hexylamine or *n*-octylamine were added to D1 gel, the chemical shift of OH proton appeared downfield to 4.37, 4.27, 4.23, 4.19, 4.17 ppm, and 4.33, 4.23, 4.20, 4.16, 4.14, ppm respectively. It was noticed that the gelator also responded to the mechanical force, which could trigger the reversible phase transitions conveniently. The thixotropic property of organogel made from D1 in several compounds used in industrial applications, including ethanol, *o*-dichlorobenzene, ANs, JP-10, was examined by step-strain measurements (ESI, Fig. S12[†]). Interestingly, all gels displayed an excellent thixotropic property, showing instant recovery of the gel state after damage and almost 100% recovery ratio of the G' values. Furthermore, the D1-based gels also exhibited self-supporting, load-bearing, and self-healing properties. As shown in Fig. S13,[†] the gels could be shaped like any free-standing objects, such as cubes and cylinders, and could preserve the shape at a weight less than 200 g. Pieces of D1/*o*-dichlorobenzene gel blocks could also be gathered into a continuous gel block within 5 min. In the light of the properties discussed above, it can be stated that the prepared gels are ideal for fabrication of multifunctional materials with versatile applications.

Hence, the D1 gels can first be used as self-constraint lubricating materials with high phase transition temperature. TGA and DSC analyses (ESI, Fig. S14[†]) indicated that the ANs gel exhibits a good thermal stability up to 200 °C, suggesting the gel lubricate has the possibility of being used at high temperature. In addition, the rheological characterization of the gels were investigated (ESI, Fig. S15[†]), it can be seen that the G' and G'' is larger than G'' within the whole frequency and strain sweep, suggesting their gel nature. Both G' and G'' kept relatively stable in the 0.1–100 rad s⁻¹ range, displaying that the ANs gel has good tolerance to external forces. The apparent viscosity test showed that the viscosity of ANs gels decreases with the shear rate increasing, which implies the pseudoplastic and shear-thinning behavior of the gel. The destroy and recovery rheological measurement showed that the G' of ANs gel could recover to their original value immediately after the cessation of the destructive strain, illustrated rapid self-healing abilities and excellent thixotropic properties. The above results showed that ANs gel has excellent thermal reversibility, good creep recovery, and thixotropic properties, endowing it with “self-restraining” properties. The lubricating properties of ANs and the corresponding D1/ANs gel at RT were investigated. As shown in Fig. 3a, the friction coefficients (COF) and wear volumes (WV) of ANs of 0.185 and 2 016 104 μm^3 , respectively, changed to 0.128 and 947 810 μm^3 , respectively, in D1/ANs gel (2 wt%). Compared with pure ANs, D1/ANs gels have lower COF and wear volumes, indicating better lubricating and anti-wear properties. Interestingly ANs gel (2 wt%) also showed stable small COF (0.152) and WV (1 314 769 μm^3) at 150 °C, suggesting excellent lubricity at high temperatures. The friction-reduction and antiwear mechanism were evaluated by a series of experiments related to ANs gel. As shown in Fig. S16 (ESI),[†] compared with pure ANs, the steel surface was eroded less severe in ANs gels. EDS elemental analysis (ESI, Fig. S17[†]) illustrates that the ANs

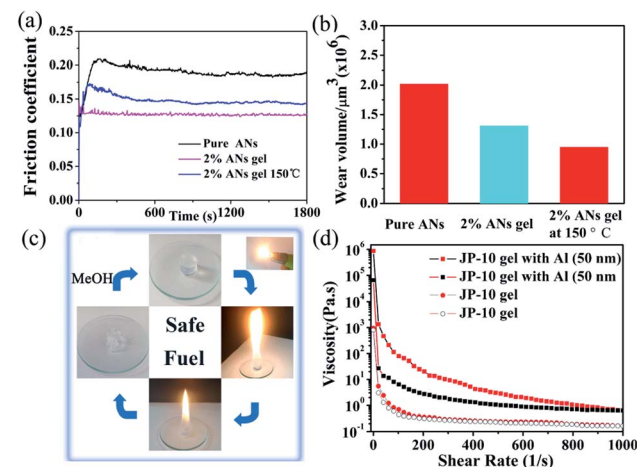


Fig. 3 (a) Evolution of the friction coefficients with time for ANs, D1/ANs gel and D1/ANs gel (2%, w/v) at 150 °C. (b) Wear volumes of steel disks lubricated by pure ANs, 2% ANs gel and 2% ANs gel (150 °C). (c) The burning methanol gel and recharge by methanol (1%, w/v). (d) Viscosity curves of 2 wt% D1 JP-10 gel with or without Al powers at shear rates ranging from 0–1000 s⁻¹.

gel could slow down the deterioration of base oil and prevent the corrosion of steel efficiently. SEM images and corresponding 3D optical microscopy (ESI, Fig. S18†) performed for the worn surfaces of steel disks indicates that ANs gel has good anticorrosion properties which could prevent corrosive wear. XPS (ESI, Fig. S19†) indicate that complicated tribochemical reactions occurred during friction. ECR indicate that a tribofilm generated on the surfaces by the tribochemical reaction. Details were observed in ESI.† Hence, the reason that ANs gel possesses excellent lubricity was proposed. First, the D1 molecules adsorb on the metal surface by polar groups during. Then a protective film composed of different iron oxides was formed on the steel surface *via* complicated triboelectrochemical reactions. The direct contact of the friction pair was obstructed by the tribofilm, which could greatly decrease the friction and wear on the steel surface, leading to a better lubricating performance.

In addition, D1 alcogels can be promising safe fuels. As shown in Fig. 3d, a piece of D1/methanol or D1/ethanol gel could be set on fire with a cigarette lighter. It is worth noticing that no shoot, smoke, unpleasing odor and ash were produced during the gel burning. The gelling agents (5 mg of D1 in 0.5 mL methanol) can burn for at least 4 min and are non-explosive, non-carcinogenic, and non-corrosive. Furthermore, the residue after burning could be reused by emerging in methanol or ethanol in a certain proportion. The cycle of burning-regeneration of the gel can be repeated several times. To study the durability of the gelator, TGA and DSC analyses were performed (ESI, Fig. S20†). The results indicated that the gelator exhibits a thermal stability up to 280 °C. On the other hand, the fuel gel could be become more colorful and attractive by adding various organic dyes (methyl violet, methyl orange or rhodamine 6G) (ESI, Fig. S21†). Therefore, the D1 alcogels can be used as a durable, recyclable, green and safe fuel. Furthermore, D1/JP-10 gels proved to be promising gel propellants, an accelerant nano powder could be introduced to improve the overall performance of the rocket engine system. The results of strain sweep tests suggested that JP-10 gel exhibits an ultrahigh mechanical strength with a storage modulus G' of 72 740 Pa. However, the gel is destroyed at a critical strain of 2% (ESI, Fig. S22†). The apparent viscosity test showed that the initial and final viscosity of JP-10 gel are 950 and 800 Pa s, respectively (Fig. 3d), which indicates the shear-thinning behavior of the JP-10 gel. To enhance the specific impulse and volumetric loading of the propellant, nano aluminum powder was added to the JP-10 gel system. Thus, aluminum powder with an average diameter of 50 nm was added to the gel system to prepare metalized JP-10 gels (5 wt% Al powders were used for 2 wt% D1). Unlike the non-metalized gel, increased storage modulus (158 000 Pa), yield stress (40.1%) and a notably large hysteresis loop were obtained for the metalized JP-10 gel (Fig. 3d and ESI, Fig. S22†). In addition, a considerable high initial viscosity of 8.71×10^5 Pa s was obtained (Fig. 3d). It is thus obvious that the metalized JP-10 gel can significantly increase the combustion performance and the rheological properties of the fuel.

We further explored the potential of D1-based gels for other practical applications. Interestingly, it was noticed that the D1 powders can spontaneously gelate up to five liquid aldehydes

from aldehyde–water mixtures at room temperature (ESI, Fig. S23†). For practical applications, 1500 mg of D1 powder was added to a mixture made of 30 mL of octanal and 300 mL of water. It was found that the aldehyde layer could be spontaneously gelled, and the solidified octanal could be easily separated by a scoop net. Octanal and D1 gelator could be separated by simple vacuum distillation, and the gelator powders could be totally reused (Fig. S24a–e†), suggesting their high potential application for the aldehydes recovery from aqueous mixtures.

In addition, D1-based xerogels showed excellent dyes adsorption capacities (ESI Fig. S25–S28†) and enhanced fluorescence properties of acid fuchsin (AF) and ciprofloxacin hydrochloride (Cipro) in aqueous solutions (Fig. S24f and g†). The addition of 1 mg of D1/acetonitrile xerogel to the aqueous solutions of acid fuchsin (8 mL, 0.1 mM) and Cipro (8 mL, 0.01 mM), the antibiotic showed obvious fluorescence under UV irradiation while the former did not show much obvious change probably due to its own color masking. However, the color of the aqueous solution of acid fuchsin became darker after exposure to the daylight (ESI Fig. S29†), and the fluorescence emission spectra further indicated the enhancement effects of D1/acetonitrile xerogels to both samples (Fig. S24h and i†).

Conclusions

In conclusion, sugar-based super gelators with multifunctional properties were prepared. These gels responded to various chemical and physical stimuli and exhibited multiple visualized molecular recognition abilities. In addition, D1-based supramolecular gels showed outstanding thixotropic, self-healing, load-bearing and moldable properties. The potential applications of the obtained materials, *i.e.* effective lubricants, safe fuels, high-efficient propellants and dyes adsorbents, were demonstrated. Particularly, D1 powders could spontaneously gel up to five aldehydes from aldehyde–water mixtures at room temperature without any assistance. Besides, D1 xerogel exhibited enhanced fluorescence emission. The outcomes of this work demonstrate that the D1-based gels could be one of the next-generations of smart soft materials.

Conflicts of interest

There are no conflicts to declare.

Acknowledgements

This research was supported by the Foundation of He'nan Educational Committee (21A530009), He'nan Provincial Natural Science Foundation (202300410502), Space Star Incubation Project (2019ZCKJ212), Shandong Provincial Natural Science Foundation (ZR2017BB019), Medical Science and Technology Development in Shandong Province (2017WS258), Shandong Province Traditional Chinese Medicine Science and Technology Development Plan (2019-0349), Scientific Research Foundation for the Doctoral Program (2014BSJJ061).

Notes and references

1 (a) O. Dumele, J. H. Chen, J. V. Passarelli and S. I. Stupp, *Adv. Mater.*, 2020, **32**, 1907247; (b) F. A. Larik, L. L. Fillbrook, S. S. Nurtila, A. D. Martin, R. P. Kuchel, K. A. Taief, M. Bhadbhade, J. E. Beves and P. Thordarson, *Angew. Chem., Int. Ed.*, 2021, **60**, 6764–6770; (c) F. Xu, L. Pfeifer, S. Crespi, F. K.-C. Leung, M. C. A. Stuart, S. J. Wezenberg and B. L. Feringa, *J. Am. Chem. Soc.*, 2021, **143**, 5990–5997.

2 (a) D. B. Amabilino, D. K. Smith and J. W. Steed, *Chem. Soc. Rev.*, 2017, **46**, 2404–2420; (b) R. G. Weiss, *J. Am. Chem. Soc.*, 2014, **136**, 7519–7530; (c) C. Chen, X. Yang, S. J. Li, C. Zhang, Y. N. Ma, Y. X. Ma, P. Gao, S. Z. Gao and X. J. Huan, *Green Chem.*, 2021, **23**, 1794–1804.

3 (a) X. W. Zhang, J. Wang, H. Jin, S. T. Wang and W. L. Song, *J. Am. Chem. Soc.*, 2018, **140**, 3186–3189; (b) L. A. J. Rutgeerts, A. H. Soultan, R. Subramani, B. Toprakhisar, H. Ramon, M. C. Paderes, W. M. D. Borggraeve and J. Patterson, *Chem. Commun.*, 2019, **55**, 7323–7326.

4 (a) J. H. Liu, J. J. Li, P. Lin, N. X. Zhang, X. Y. Han, B. Zhan and J. Song, *Chem. Commun.*, 2016, **52**, 13975–13978; (b) W. D. Wang, L. Xiang, L. Gong, W. J. Hu, W. J. Huang, Y. J. Chen, A. B. Asha, S. Srinivas, L. Y. Chen, R. Narain and H. B. Zeng, *Chem. Mater.*, 2019, **31**, 2366–2376.

5 (a) D. Gambhir, S. Kumar, G. Dey, V. Krishnan and R. R. Koner, *Chem. Commun.*, 2018, **54**, 11407–11410; (b) X. B. Xu, J. N. Xiao, M. Y. Liu and Z. I. Liu, *Chem. Commun.*, 2019, **55**, 14178–14181; (c) K. Q. Fan, X. B. Wang, Z. G. Yin, C. J. Jia, B. H. Zhang, L. M. Zhou and J. Song, *J. Mater. Chem. C*, 2018, **6**, 10192–10196.

6 (a) S. Datta, S. Samanta and D. Chaudhuri, *J. Mater. Chem. A*, 2018, **6**, 2922–2926; (b) C. L. Ren, J. Shen, F. Chen and H. Q. Zeng, *Angew. Chem., Int. Ed.*, 2017, **56**, 3847–3851.

7 (a) P. Pallavi, S. Bandyopadhyay, J. Louis, A. Deshmukha and A. Patra, *Chem. Commun.*, 2017, **53**, 1257–1260; (b) X. Y. Han, J. H. Liu, C. Y. Zhao, B. Zhang, X. F. Xu and J. Song, *J. Colloid Interface Sci.*, 2018, **525**, 177–186.

8 S. Bera and D. Haldar, *J. Mater. Chem. A*, 2016, **4**, 6933–6939.

9 Y. R. Wang, Q. L. Yu, Y. Y. Bai, L. Q. Zhang, F. Zhou, W. M. Liu and M. R. Cai, *ACS Sustainable Chem. Eng.*, 2018, **6**, 15801–15810.

10 A. Q. Chen, X. D. Guan, X. M. Li, B. H. Zhang, B. Zhang and J. Song, *Propellants, Explos., Pyrotech.*, 2017, **42**, 1007–1013.

11 B. O. Okesola and D. K. Smith, *Chem. Soc. Rev.*, 2016, **45**, 4226–4251.

12 (a) J. P. Wojciechowski, A. D. Martin and P. Thordarson, *J. Am. Chem. Soc.*, 2018, **140**(8), 2869–2874; (b) T. Guterman, M. Levin, S. Kolusheva, D. Levy, N. Noor, Y. Roichman and E. Gazit, *Angew. Chem., Int. Ed.*, 2019, **56**, 15869–15875.

13 W. R. Chen, G. Y. Qing and T. L. Sun, *Chem. Commun.*, 2017, **53**, 447–450.

14 Z. Horváth, B. Gyarmati, A. Menyhárd, P. Doshev, M. Gahleitner, J. Varga and B. Pukánszky, *RSC Adv.*, 2014, **4**, 19737–19745.

15 S. Y. Dong, B. Zheng, D. H. Xu, X. Z. Yan, M. M. Zhang and F. H. Huang, *Adv. Mater.*, 2012, **24**, 3191–3195.

16 S. Mondal, P. Bairi, S. Das and A. K. Nand, *J. Mater. Chem. A*, 2019, **7**, 381–392.

17 W. Zheng, L. J. Chen, G. Yang, B. Sun, X. Wang, B. Jiang, G. Q. Yin, L. Zhang, X. P. Li, M. H. Liu, G. S. Chen and H. B. Yang, *J. Am. Chem. Soc.*, 2016, **138**, 4927–4937.

18 Z. C. Shen, Y. Q. Jiang, T. Y. Wang and M. H. Liu, *J. Am. Chem. Soc.*, 2015, **137**, 16109–16115.

19 (a) J. J. Li, K. Q. Fan, X. D. Guan, Y. Z. Yu and J. Song, *Langmuir*, 2014, **30**, 13422–13429; (b) B. O. Okesola, V. M. P. Vieira, D. J. Cornwell, N. K. Whitelaw and D. K. Smith, *Soft Matter*, 2015, **11**, 4768–4787.

20 X. H. Zhang, H. M. Li, X. Zhang, M. An, W. W. Fang and H. T. Yu, *Front. Chem. Eng.*, 2017, **11**, 231–237.

